

Effects of Acceptance of Enlightenment on COVID-19 Transmission using Homotopy Perturbation Method

Tawakalt Abosede Ayoola, Mutairu Kayode Kolawole, and Amos Oladele Popoola



Volume 3, Issue 2, Pages 39–48, December 2022

Received 10 August 2022, Accepted 17 November 2022, Published Online 31 December 2022

To Cite this Article : T. A. Ayoola, M. K. Kolawole, and A. O. Popoola, "Effects of Acceptance of Enlightenment on COVID-19 Transmission using Homotopy Perturbation Method", *Jambura J. Biomath*, vol. 3, no. 2, pp. 39–48, 2022, <https://doi.org/10.34312/jjbm.v3i2.15798>

© 2022 by author(s)

JOURNAL INFO • JAMBURA JOURNAL OF BIOMATHEMATICS



	Homepage	:	http://ejurnal.ung.ac.id/index.php/JJBM/index
	Journal Abbreviation	:	Jambura J. Biomath.
	Frequency	:	Biannual (June and December)
	Publication Language	:	English (preferable), Indonesia
	DOI	:	https://doi.org/10.34312/jjbm
	Online ISSN	:	2723-0317
	Editor-in-Chief	:	Hasan S. Panigoro
	Publisher	:	Department of Mathematics, Universitas Negeri Gorontalo
	Country	:	Indonesia
	OAI Address	:	http://ejurnal.ung.ac.id/index.php/jjbm/oai
	Google Scholar ID	:	XzYgeKQAAAAJ
	Email	:	editorial.jjbm@ung.ac.id

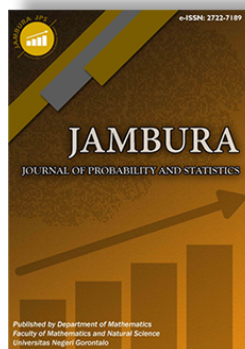
JAMBURA JOURNAL • FIND OUR OTHER JOURNALS



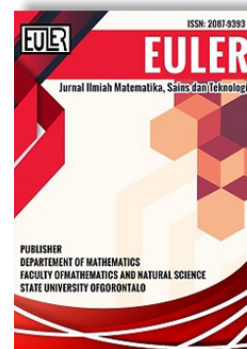
Jambura Journal of Mathematics



Jambura Journal of Mathematics Education



Jambura Journal of Probability and Statistics



EULER : Jurnal Ilmiah Matematika, Sains, dan Teknologi

Effects of Acceptance of Enlightenment on COVID-19 Transmission using Homotopy Perturbation Method

Tawakalt Aboosedo Ayoola^{1,*}, Mutairu Kayode Kolawole²,
and Amos Oladele Popoola³

^{1,2,3}Department of Mathematical Sciences, Faculty of Basic and Applied Sciences, Osun State University, Osogbo, Nigeria

ARTICLE HISTORY

Received 10 August 2022
Accepted 17 November 2022
Published 31 December 2022

KEYWORDS

COVID-19
global Stability
enlightenment
Homotopy
Perturbation Method

ABSTRACT. The deadly Corona virus disease has had a significantly devastating impact on the general public, necessitating the study of transmission dynamics. A mathematical model of a non-linear differential equation for COVID-19 infection is investigated with the effects of some basic factors, such as the acceptance of enlightenment to avoid being exposed and the acceptance of enlightenment to go for vaccination. The basic reproduction number, which determines the disease's spread, is calculated. The local and global stability analyses of the model are carried out. The sensitivity analysis is also computed. Numerical simulation using the homotopy perturbation method demonstrates the effect of the acceptance of enlightenment on the population. Our results indicate that when the populace accepts vaccination, the rate at which COVID-19 spreads reduces.



This article is an open access article distributed under the terms and conditions of the Creative Commons Attribution-NonCommercial 4.0 International License. *Editorial of JJBM:* Department of Mathematics, Universitas Negeri Gorontalo, Jln. Prof. Dr. Ing. B. J. Habibie, Bone Bolango 96554, Indonesia.

1. Introduction

A worldwide outbreak of COVID-19 has taken hold. New coronavirus hotspots have been identified in Wuhan, China, in December 2019. When a large number of people were admitted to the hospital in the latter days of December 2019, it was clear that the epidemic had begun. Pneumonia was discovered in these people [1]. At first, physicians in Wuhan, China's Hubei Province, suspected a seafood and wet animal market was to blame. According to the World Health Organization (WHO), Coronavirus Disease 2019 (COVID) is caused by the virus Severe Acute Respiratory Syndrome Coronavirus 2, which is also known as SARS-CoV-2 [2]. In March 2020, the World Health Organization (WHO) proclaimed the COVID-19 pandemic. World Health Organization (WHO), 2020a. It was confirmed on February 27, 2020, in Nigeria that the index case had been established. the establishment of a multi-sectoral Emergency Operations Center by the Nigerian Center for Disease Control (EOC). with a total of 11,516 cases and 323 deaths [2].

Numerous hypotheses have been put forth by professionals to explain COVID-19's peculiar behaviors. It was found that a mathematical model established by [3] included undiagnosed infectious cases, hospital sensitization conditions, and a proportion of known cases. Using a mathematical model, [4] investigated how mask use affects the general public. [5] presented a new mathematical model of COVID-19 that accounts for the effects of the first and second doses of vaccination. The basic reproduction number that represents an epidemic indicator was obtained, and the stability analysis criteria were determined. The study concluded that the double-dose vaccination was recommended as the best way to curb the spread of COVID-19. Also,

researchers like [6] studied the impact of COVID-19 infections on social interactions. It was shown that social awareness and speedy testing had an impact on a COVID-19 transmission model [7]. The research takes into consideration both known and unknown COVID-19 infections in the exposed phase of infection. [8] studied the influence of public awareness efforts on the dynamics of COVID-19 infection.

Furthermore, one of the semi-analytical techniques for solving linear and nonlinear ordinary differential equations is the homotopy perturbation method. Several researchers now use numerical techniques such as the Adomian Decomposition Method established by [9], the Variational Iteration Method introduced by [10], and the Homotopy Perturbation Method introduced by [11] to obtain their approximate solution. Authors like [12] used the homotopy perturbation method to analyze the Equine Infectious Anemia Virus (EIAV) model. [13] used the homotopy perturbation method to obtain an approximate solution to the fractional-order integral-differential equation. Their results converge faster to the exact solution when compared to other numerical methods. [14] discussed the future condition of COVID-19 in Bangladesh by analyzing the current situation with an SIR model according to the present data for Bangladesh.

The research into an effective COVID-19 vaccination continues apace. A new mathematical model of the COVID-19 pandemic, including the vaccination campaign, was studied by [20]. The World Health Organization (WHO) Strategic Advisory Group of Experts on Immunization (SAGE) defined vaccine hesitancy as a delay in acceptance or refusal of vaccination despite the availability of vaccination services. According to [21], who carried out a cross-sectional survey on health students on the determinants of COVID-19 vaccine acceptance and hesitancy, the results

*Corresponding Author.

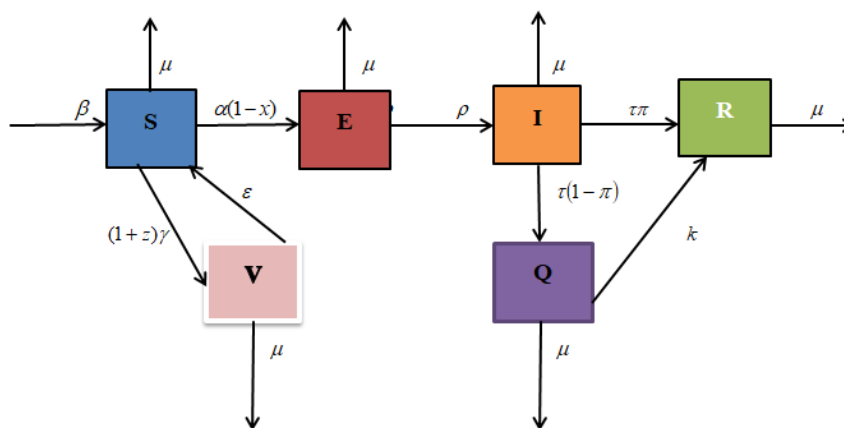


Figure 1. Schematic Picture of the proposed COVID-19 model

Table 1. Detailed description of the Model

Parameters	Description	Values	References
β	Recruitment rate	68,597.853	Estimated
α	Transmission rate	0.09091	Jumanne et al. [15]
ϵ	Wane rate of vaccine	0.25	Assumed
ρ	Exit rate from Exposed class	0.13	Tang et al. [16]
τ	Exit rate from Infectious class	0.0833	Babaei et al. [17]
π	Proportion of infectious who recovered naturally	0.05	Deressa et al. [18]
x	Acceptance of enlightenment to avoid being exposed	0.2	Assumed
z	Acceptance of enlightenment to go for vaccination	0.3	Assumed
μ	Natural Death rate	0.0003205128	Estimated
δ	Covid-19 Induced death rate	0.018	Garba et al. [19]
k	Recovery rate of Quarantine Individuals	0.0701	Garba et al. [19]
γ	Vaccination rate	0.4	Assumed

show that 491 (77.81%) students actually received the COVID-19 vaccine, and of the 140 unvaccinated, 69 were hesitant and 71 rejected it. The goal of this study is to present the use of the homotopy perturbation method to examine the impact of acceptances of enlightenment on the entire population in order to avoid being exposed to COVID-19 and to enlighten them to go for vaccination.

2. Model Formulation

A mathematical model of the COVID-19 mode of transmission has been developed, with the population under investigation divided into six divisions, depending on the epidemiological state of each person in the population, there are Susceptible sections $S(t)$; Vaccinated $V(t)$; Exposed class $E(t)$; Infected class $I(t)$; Quarantine class $Q(t)$; Recovered class $R(t)$; The entire human population $N(t)$ is calculated as follows:

$$N(t) = S(t) + V(t) + E(t) + I(t) + Q(t) + R(t).$$

The model is SVEIQR not SVEIQRS, which implies that anybody in recovered class are assumed to have permanent immunity. Hence, the rate at which the susceptible class is recruited is by immigration or birth at β , and the force of infection $\lambda = \alpha SI$, where α denotes the effective transmission rate between susceptible and infectious people, and ρ , denotes the rate of progression from exposed to infected. Let x be the rate of acceptance

of enlightenment to avoid being exposed, while z is the rate of acceptance of enlightenment to go for vaccination. The vaccination rate is γ and wane rate of vaccine is ϵ . Let τ be the rate of exit from Infected class to quarantine, in which a proportion $(1 - \pi)$ is quarantined and a proportion π is naturally recovered. The quarantine individuals are treated and recovered at a rate k , natural death occurs in all six classes at a rate μ , and death from COVID -19 occurs at a rate δ . Thus, we have the following nonlinear differential equation systems.

$$\begin{aligned} \frac{dS}{dt} &= \beta - \alpha(1-x)SI - (1+z)\gamma S - \mu S + \epsilon V = g_1 \\ \frac{dV}{dt} &= (1+z)\gamma S - (\epsilon + \mu)V = g_2 \\ \frac{dE}{dt} &= \alpha(1-x)SI - (\mu + \rho)E = g_3 \\ \frac{dI}{dt} &= \rho E - (\mu + \delta + \tau)I = g_4 \\ \frac{dQ}{dt} &= \tau(1-\pi)I - (\mu + \delta + k)Q = g_5 \\ \frac{dR}{dt} &= \tau\pi I + kQ - \mu R = g_6. \end{aligned} \tag{1}$$

The schematic diagram of the model (1) is given by Figure 1 and its biological parameters are given by Table 1.

Remark 1. (i) For $0 \leq x \leq 1$, when $x = 0$ infers that either the susceptible people are not informed or that the educational effort has no effect on the level of COVID-19 exposure.
 (ii) For $0 \leq z \leq 1$, when $z = 0$ it indicates that the susceptible individuals have not been immunized or that the vaccine has had no impact on them.

3. Model Analysis

3.1. Existence and Uniqueness of Solution

A Lipchitz criterion will be used to check for the existence and uniqueness of solution. For $g_1 = \beta - \alpha(1-x)SI - (1+z)\gamma S - \mu S + \varepsilon V$, we have

$$\begin{aligned} \left| \frac{dg_1}{dS} \right| &= |-\alpha(1-x)I - (1+z)\gamma - \mu|, \\ \left| \frac{dg_1}{dV} \right| &= |\varepsilon|, \quad \left| \frac{dg_1}{dE} \right| = 0, \\ \left| \frac{dg_1}{dI} \right| &= |-\alpha(1-x)S|, \quad \left| \frac{dg_1}{dQ} \right| = 0, \quad \left| \frac{dg_1}{dR} \right| = 0. \end{aligned} \tag{2}$$

For $g_2 = (1+z)\gamma S - (\varepsilon + \mu)V$, we get

$$\begin{aligned} \left| \frac{dg_2}{dS} \right| &= |(1+z)\gamma|, \quad \left| \frac{dg_2}{dV} \right| = |-\varepsilon - \mu|, \\ \left| \frac{dg_2}{dE} \right| &= 0, \quad \left| \frac{dg_2}{dI} \right| = 0, \quad \left| \frac{dg_2}{dQ} \right| = 0, \quad \left| \frac{dg_2}{dR} \right| = 0. \end{aligned} \tag{3}$$

For $g_3 = \alpha(1-x)SI - (\rho + \mu)E$, we obtain

$$\begin{aligned} \left| \frac{dg_3}{dS} \right| &= |\alpha(1-x)I|, \quad \left| \frac{dg_3}{dV} \right| = 0, \quad \left| \frac{dg_3}{dE} \right| = |-\rho - \mu|, \\ \left| \frac{dg_3}{dI} \right| &= |\alpha(1-x)S|, \quad \left| \frac{dg_3}{dQ} \right| = 0, \quad \left| \frac{dg_3}{dR} \right| = 0. \end{aligned} \tag{4}$$

For $g_4 = \rho E - (\mu + \tau + \delta)I$, we acquire

$$\begin{aligned} \left| \frac{dg_4}{dS} \right| &= 0, \quad \left| \frac{dg_4}{dV} \right| = 0, \quad \left| \frac{dg_4}{dE} \right| = |\rho|, \\ \left| \frac{dg_4}{dI} \right| &= |-\mu - \tau - \delta|, \quad \left| \frac{dg_4}{dQ} \right| = 0, \quad \left| \frac{dg_4}{dR} \right| = 0. \end{aligned} \tag{5}$$

For $g_5 = \tau(1-\pi)I - (\mu + k + \delta)Q$, we have

$$\begin{aligned} \left| \frac{dg_5}{dS} \right| &= 0, \quad \left| \frac{dg_5}{dV} \right| = 0, \quad \left| \frac{dg_5}{dE} \right| = 0, \\ \left| \frac{dg_5}{dI} \right| &= |\tau(1-\pi)|, \quad \left| \frac{dg_5}{dQ} \right| = |-\mu - k - \delta|, \quad \left| \frac{dg_5}{dR} \right| = 0. \end{aligned} \tag{6}$$

Again, for $g_6 = \tau\pi I + kQ - \mu R$, we finally get

$$\begin{aligned} \left| \frac{dg_6}{dS} \right| &= 0, \quad \left| \frac{dg_6}{dV} \right| = 0, \quad \left| \frac{dg_6}{dE} \right| = 0, \quad \left| \frac{dg_6}{dI} \right| = \tau\pi, \\ \left| \frac{dg_6}{dQ} \right| &= |k|, \quad \left| \frac{dg_6}{dR} \right| = |-\mu|. \end{aligned} \tag{7}$$

These partial derivatives exist are continuous and are bounded, therefore the model (1) exist and has a unique solution in \mathbb{R}^6 .

3.2. Invariant Region

Lemma 1. For $t \geq 0$, all variables and parameters are assumed to be nonnegative. We demonstrate that the area where the model is sensible is positively invariant and appealing to the model for all $t \geq 0$, such that all the solution in Ω remains in Ω for all $t \geq 0$.

Proof. Recall that, the entire human population is defined as $N(t) = S(t) + V(t) + E(t) + I(t) + Q(t) + R(t)$ since human population changes in terms of time

$$\begin{aligned} \frac{dN}{dt} &= \frac{dS}{dt} + \frac{dV}{dt} + \frac{dE}{dt} + \frac{dI}{dt} + \frac{dQ}{dt} + \frac{dR}{dt} \\ &= \beta - \alpha(1-x)SI - (1+z)\gamma S - \mu S + \varepsilon V \\ &\quad + (1+z)\gamma S - \varepsilon V - \mu V + \alpha(1-x)SI - \rho E \\ &\quad - \mu E + \rho E - \mu I - \tau I - \delta I + \tau I - \tau\pi I - \mu Q \\ &\quad - kQ + \delta Q + \tau\pi I + kQ - \mu R \\ &= \beta - \mu(S + V + E + I + Q + R) - \delta(I + Q). \end{aligned}$$

In the absence of COVID-19 induced death ($\delta = 0$), the above equation becomes

$$\frac{dN}{dt} = \beta - \mu N \tag{8}$$

Integrating both side of eq. (8), we have that

$$\begin{aligned} \int_0^t \frac{dN}{\beta - \mu N} &\leq \int_0^t dt \\ -\frac{1}{\mu} \ln(\beta - \mu N) &\leq t \end{aligned} \tag{9}$$

From eq. (9) we have

$$N \leq \frac{\beta}{\mu} - \left[\frac{\beta - \mu N_0}{\mu} \right] e^{-\mu t}$$

As $t \rightarrow \infty$ we have $N \leq \frac{\beta}{\mu}$. This implies that the proposed model (1) can be studied in the feasible region

$$\Omega = \left\{ (S, V, E, I, Q, R) \in \mathbb{R}^6 : N \leq \frac{\beta}{\mu} \right\}$$

□

3.3. Positivity of Solution

Theorem 1. Given $S > 0, V \geq 0, E \geq 0, I \geq 0, Q \geq 0$ and $R \geq 0$. Then the solution

$$\left\{ (S, V, E, I, Q, R) \in \mathbb{R}^6 : N \leq \frac{\beta}{\mu} \right\}$$

are positive invariant for $t \geq 0$.

Proof. Recall, based on the initial equation (1) by introducing the force of infection λ for simplicity of the expression then:

$$\begin{aligned} \frac{dS(t)}{dt} &\geq -(\lambda(1-x) + (1+z)\gamma + \mu) \\ \frac{dS(t)}{S(t)} &\geq -(\lambda(1-x) + (1+z)\gamma + \mu) dt \end{aligned}$$

$$\frac{dS(t)}{S(t)} \geq \int -(\lambda(1-x) + (1+z)\gamma + \mu) dt.$$

By solving using method of separation of variable and also applied the initial condition, we have

$$S(t) \geq S_0 e^{-(\lambda(1-x) + (1+z)\gamma + \mu)t} \geq 0. \tag{10}$$

Repeating the same procedure for the rest of the equations we obtain

$$\begin{aligned} V(t) &\geq V_0 e^{-(\varepsilon + \mu)t} \geq 0, \\ E(t) &\geq E_0 e^{-(\mu + \rho)t} \geq 0, \\ Q(t) &\geq Q_0 e^{-(\mu + \delta + k)t} \geq 0, \\ R(t) &\geq R_0 e^{-\mu t} \geq 0. \end{aligned}$$

Obviously, the solution of the model is positive. This completes the proof of the theorem. \square

Having satisfied all the basic properties of an epidemiology model, we conclude that the proposed model is suitable to study COVID-19 in human population.

3.4. Existence of Disease-Free Equilibrium and Basic Reproduction Number (R_0).

The disease-free equilibrium point of the model (1) can be found by setting $E = I = 0$. Hence, the disease free equilibrium point is obtained by

$$\begin{aligned} T^0 &= (S^0, V^0, E^0, I^0, Q^0, R^0) \\ &= \left(\frac{\beta(\varepsilon + \mu)}{\mu(\gamma z + \gamma + \mu + \varepsilon)}, \frac{(1+z)\gamma\beta}{\mu(\gamma z + \gamma + \mu + \varepsilon)}, 0, 0, 0, 0 \right) \end{aligned} \tag{11}$$

Basic Reproduction Number

Diekmann and Heesterbeek [22] define the basic reproduction number, commonly denoted by R_0 , as the average number of secondary infections induced by a typical infectious person during the duration of his or her infectious period. F is the rate of appearance of new infections in compartment i , V_i^+ is the rate of transfer of individuals into the compartment by all other means. V_i^- is the rate of transfer of individuals out of the compartment, such that $V = V^- - V^+$. In this section, we'll consider three different types of equations:

$$\begin{aligned} \dot{E} &= \alpha(1-x)SI - (\rho + \mu)E \\ \dot{I} &= \rho E - (\mu + \tau + \delta)I \\ \dot{Q} &= \tau(1-\pi)I - (\mu + k + \delta)Q \end{aligned} \tag{12}$$

From the above equation, we obtained

$$\begin{aligned} F &= \begin{bmatrix} 0 & \alpha(1-x)S & 0 \\ 0 & 0 & 0 \\ 0 & 0 & 0 \end{bmatrix} \\ F_{DFE} &= \begin{bmatrix} 0 & \alpha(1-x)S^0 & 0 \\ 0 & 0 & 0 \\ 0 & 0 & 0 \end{bmatrix} \end{aligned}$$

$$\begin{aligned} V &= \begin{bmatrix} (\rho + \mu) & 0 & 0 \\ -\rho & (\mu + \tau + \delta) & 0 \\ 0 & -\tau(1-\pi) & (\mu + k + \delta) \end{bmatrix} \\ V^{-1} &= \begin{bmatrix} \frac{1}{(\rho + \mu)} & 0 & 0 \\ \frac{\rho}{(\rho + \mu)(\mu + \tau + \delta)} & \frac{1}{(\mu + \tau + \delta)} & 0 \\ \frac{\rho\tau(1-\pi)}{(\rho + \mu)(\mu + \tau + \delta)(\mu + k + \delta)} & \frac{\tau(1-\pi)}{(\mu + \tau + \delta)(\mu + k + \delta)} & \frac{1}{(\mu + k + \delta)} \end{bmatrix}. \end{aligned}$$

Since, $R_0 = FV^{-1}$ we have

$$FV^{-1} = \begin{bmatrix} \frac{\alpha(1-x)S^0\rho}{(\rho + \mu)(\mu + k + \delta)} & \frac{\alpha(1-x)S^0}{(\mu + k + \delta)} & 0 \\ 0 & 0 & 0 \\ 0 & 0 & 0 \end{bmatrix}$$

The basic reproduction number R_0 is obtained by taking the largest (dominant) eigenvalue or spectral radius of $\rho(FV^{-1})$.

$$R_0 = \frac{\alpha(1-x)S^0\rho}{(\rho + \mu)(\mu + \tau + \delta)}$$

Such that

$$S^0 = \frac{\beta(\mu + \varepsilon)}{\mu(\gamma z + \gamma + \mu + \varepsilon)}$$

Therefore

$$R_0 = \frac{\alpha(1-x)\beta\rho(\mu + \varepsilon)}{(\rho + \mu)(\mu + \tau + \delta)\mu(\gamma z + \gamma + \mu + \varepsilon)}. \tag{13}$$

3.5. Local Stability Analysis of Diseases Free Equilibrium

The following outcomes are demonstrated while studying the stability of the model's equilibria.

Lemma 2. The model's disease-free equilibrium is locally asymptotically stable if $R_0 < 1$, otherwise, it is unstable if $R_0 > 1$.

Proof. We look at the system's Jacobian of the model (1) which is given by

$$J(T^0) = \begin{bmatrix} -(1+z)\gamma - \mu & \varepsilon & 0 & -X & 0 & 0 \\ (1+z)\gamma & -\mu - \varepsilon & 0 & 0 & 0 & 0 \\ 0 & 0 & -\rho - \mu & X & 0 & 0 \\ 0 & 0 & \rho & -\delta - \mu - \tau & 0 & 0 \\ 0 & 0 & 0 & \tau(1-\pi) & -\mu - \delta - k & 0 \\ 0 & 0 & 0 & \tau\pi & k & -\mu \end{bmatrix}$$

Where

$$X = \frac{\alpha(1-x)\beta(\mu + \varepsilon)}{\mu(\gamma z + \gamma + \mu + \varepsilon)}$$

The four eigenvalues are negative: $-\mu, -\mu, -\gamma z - \gamma - \mu - \varepsilon, -\mu - k - \delta$. The remaining two eigenvalues are given in the form of 2 by 2 matrix

$$\begin{bmatrix} -\rho - \mu & \alpha(1-x)S^0 \\ \rho & -\tau - \delta - \mu \end{bmatrix}$$

Characteristics polynomial is $\lambda^2 + a_1\lambda + a_2$, where

$$\begin{aligned} a_1 &= \rho + 2\mu + \delta + \tau \\ a_2 &= (\rho + \mu)(\delta + \mu + \tau)\mu(\gamma z + \gamma + \mu + \varepsilon)[1 - R_0] \end{aligned}$$

Thus, last two of eigenvalues are negative if $a_2 > 0$ which is attain if $R_0 < 1$. Therefore, the disease-free equilibrium is asymptotically stable locally. \square

3.6. Existence of Endemic Equilibrium State

The endemic equilibrium point of the model (1) is discovered when $S \neq V \neq E \neq I \neq Q \neq R \neq 0$. Hence the endemic equilibrium point is given by $T^* = (S^*, V^*, E^*, I^*, Q^*, R^*)$ where

$$\begin{cases} S^* = \frac{g_4 g_5}{\alpha \rho g_1}, \\ V^* = \frac{g_3 g_4 g_5}{\alpha \rho g_1 g_2}, \\ E^* = \frac{g_5 g_8 (R_0 - 1) + g_3 g_5 (\varepsilon + 1)}{\alpha \rho g_1 g_2}, \\ I^* = \frac{g_8 (R_0 - 1) + g_3 (\varepsilon + 1)}{\alpha g_1 g_2}, \\ Q^* = \frac{g_7 g_8 (R_0 - 1) + g_3 g_7 (\varepsilon + 1)}{\alpha g_1 g_2 g_6}, \\ R^* = \frac{(\tau \pi g_6 - k g_7) [g_8 (R_0 - 1) + g_3 (\varepsilon + 1)]}{\alpha \mu g_1 g_2 g_6}. \end{cases} \tag{14}$$

Where $g_1 = (1 - x)$, $g_2 = (\varepsilon + \mu)$, $g_3 = (1 + z)\gamma$, $g_4 = (\rho + \mu)$, $g_5 = (\tau + \mu + \delta)$, $g_6 = (\mu + \delta + k)$, $g_7 = \tau(1 - \pi)$, $g_8 = \mu(\mu + \gamma z + \gamma + \varepsilon)$. Equation (14) shows that if $R_0 > 1$, then the endemic equilibrium $T^*(S^*, V^*, E^*, I^*, Q^*, R^*) \in D$.

3.7. Local Stability Analysis of Endemic Equilibrium

Lemma 3. The endemic equilibrium T^* is locally asymptotically stable if $R_0 > 1$.

Proof. We consider the Jacobian of the model (1) at $T^* = (S^*, V^*, E^*, I^*, Q^*, R^*)$ which is given by

$$J(T^*) = \begin{bmatrix} A & \varepsilon & 0 & -\alpha(1-x)S^* & 0 & 0 \\ (1+z)\gamma & -\mu - \varepsilon & 0 & 0 & 0 & 0 \\ \alpha(1-x)I^* & 0 & -\rho - \mu & \alpha(1-x)S^* & 0 & 0 \\ 0 & 0 & \rho & -\delta - \mu - \tau & 0 & 0 \\ 0 & 0 & 0 & \tau(1-\pi) & -\mu - \delta - k & 0 \\ 0 & 0 & 0 & \tau\pi & k & -\mu \end{bmatrix}$$

Let $A = -\alpha(1-x)I^* - (1+z)\gamma - \mu$, the characteristics equation from $\det(J(T^*) - \lambda I) = 0$ is $(\lambda + \mu)(\lambda + \mu + \delta + k)(\lambda + \mu + \delta + \tau)(\lambda^3 + a_2\lambda^2 + a_1\lambda + a_0) = 0$, where

$$\begin{aligned} a_2 &= 3\mu + \rho + \varepsilon + \alpha(1-x)I^* + \gamma(1+z) \\ a_1 &= \alpha(1+x)I^*(2\mu + \varepsilon + \rho) + 3\mu^2 \\ &\quad + 2\mu(\gamma z + \gamma + \varepsilon + \rho) + \gamma\rho(1+z) + \rho\varepsilon \\ a_0 &= (\rho + \mu)[\alpha(1+x)I^*(\varepsilon + \mu) + \mu(\mu + \gamma z + \gamma + \varepsilon)] \\ &= (\rho + \mu)[\mu(\mu + \gamma z + \gamma + \varepsilon)(R_0 - 1) \\ &\quad + (1+z)(\gamma + \varepsilon\gamma) + \mu(\mu + \gamma z + \gamma + \varepsilon)] \\ a_2 a_1 - a_0 &= [3\mu + \rho + \varepsilon + \alpha(1-x)I^* + \gamma(1+z)] \\ &\quad [\alpha(1+x)I^*(2\mu + \varepsilon + \rho) + 3\mu^2 \\ &\quad + 2\mu(\gamma z + \gamma + \varepsilon + \rho) + \gamma\rho(1+z) + \rho\varepsilon] - \\ &\quad [(\rho + \mu)[\alpha(1+x)I^*(\varepsilon + \mu) + \mu(\mu + \gamma z + \gamma + \varepsilon)]] \\ &> 0 \end{aligned}$$

$$\begin{aligned} &\Rightarrow [3\mu + \rho + \varepsilon + \alpha(1-x)I^* + \gamma(1+z)][\alpha(1+x)I^*(2\mu + \varepsilon + \rho) \\ &\quad + 3\mu^2 + 2\mu(\gamma z + \gamma + \varepsilon + \rho) + \gamma\rho(1+z) + \rho\varepsilon] > \\ &\quad [(\rho + \mu)[\alpha(1+x)I^*(\varepsilon + \mu) + \mu(\mu + \gamma z + \gamma + \varepsilon)]] \end{aligned}$$

It is easy to verify that $a_2 > 0$, $a_1 > 0$, $a_0 > 0$ and $a_2 a_1 > a_0$ if $I^* > 0$, from eq. (14) it is clear that I^* is positive if $R_0 > 1$. Therefore, by the Routh-Hurwitz stability criterion, the Endemic Equilibrium point T^* of the model (1) is locally asymptotically stable for $R_0 > 1$. \square

3.8. Global Stability of Disease Free and Endemic Equilibria

The Castillo-Chavez approach is used to demonstrate global stability [23]. Consider a model of the form:

$$\left. \begin{aligned} \frac{dF}{dt} &= F(x, Y) \\ \frac{dI}{dt} &= G(x, Y), G(x, 0) = 0 \end{aligned} \right\} \tag{15}$$

Where $x \in \mathbb{R}^m$ represents individuals that are not infected in the population and $Y \in \mathbb{R}^n$ represent infected individuals. Following the above representation, it is possible to express the disease-free equilibrium of this system as $T^0 = (x^*, 0)$. The following two conditions (H_1) and (H_2) below must be met to guarantee global asymptotic stability.

(H_1) For $\frac{dx}{dt} = F(x, 0)$, x^* is globally asymptotically stable.

(H_2) $G(x, Y) = AY - \hat{G}(x, Y)$, $\hat{G}(x, Y) \geq 0$ for $(x, Y) \in \Omega$, where $A = D_Y G(x^*, 0)$ is an M-matrix (the off-diagonal components of A are nonnegative), and Ω is where the model makes biological sense. If system (15) satisfies the above two conditions, then the following theorems hold:

Lemma 4. [23] The fixed point $T^0 = (x^*, 0)$ is globally asymptotically stable (g.a.s) equilibrium of (15) provided that $R_0 \leq 1$ and assumption that (H_1) and (H_2) are satisfied.

Theorem 2. The DFE T^0 of the model (1) is globally asymptotically stable if $R_0 < 1$.

Proof. The model (1) above is re-written as in form of (15) by setting $x = (S, V)$,

$$\begin{aligned} Y &= (E, I, Q, R), \\ T^0 &= (x^*, 0) \\ &= \left(\frac{\beta(\varepsilon + \mu)}{\mu(\gamma z + \gamma + \mu + \varepsilon)}, \frac{(1+z)\gamma\beta}{\mu(\gamma z + \gamma + \mu + \varepsilon)}, 0 \right) \end{aligned}$$

And the system $\frac{dx}{dt} = F(x, 0)$ becomes

$$\begin{cases} \dot{S} = \beta - (1+z)\gamma S - \mu S + \varepsilon V \\ \dot{V} = (1+z)\gamma S - (\varepsilon + \mu)V \end{cases}$$

This equation has a unique equilibrium point are

$$x^* = \left(\frac{\beta(\varepsilon + \mu)}{\mu(\gamma z + \gamma + \mu + \varepsilon)}, \frac{(1+z)\gamma\beta}{\mu(\gamma z + \gamma + \mu + \varepsilon)} \right),$$

which is asymptotically stable, therefore (H1) is satisfied. For (H2) can be verified. The model (1) has

$$G(x, Y) = \begin{bmatrix} \alpha(1-x)SI - (\rho + \mu)E \\ \rho E - (\mu + \tau + \delta)I \\ \tau(1-\pi)I - (\mu + k + \delta)Q \\ \tau\pi I + kQ - \mu R \end{bmatrix}$$

$$D_Y G(x^*, 0) = \begin{bmatrix} -\mu - \rho & \alpha(1-x)S & 0 & 0 \\ \rho & -\delta - \mu - \tau & 0 & 0 \\ 0 & \tau(1-\pi) & -\delta - k - \mu & 0 \\ 0 & \tau\pi & k & -\mu \end{bmatrix}$$

Clearly, $A = D_Y G(x^*, 0)$ is a M-Matrix, On the other hand,

$$\Rightarrow \hat{G}(x, Y) = AY - G(x, Y) = \begin{pmatrix} 0 \\ 0 \\ 0 \\ 0 \end{pmatrix} \quad (16)$$

Hence, $\hat{G}(x, Y) = 0$ for all $(x, Y) \in \Omega$, therefore conditions (H1) and H2 are satisfied. With Lemma 4, the global stability of DFE is obtained and which complete the proof. \square

Theorem 3. If $R_0 > 1$, the global asymptotically stable of endemic equilibrium point of the model (1) is found.

Proof. In order to prove that the model's endemic equilibrium is globally stable, we use a Lyapunov function.

$$V(S^*, V^*, E^*, I^*, Q^*, R^*) = \begin{aligned} & \left(S - S^* - S^* \ln \frac{S}{S^*} \right) + \left(V - V^* - V^* \ln \frac{V}{V^*} \right) \\ & + \left(E - E^* - E^* \ln \frac{E}{E^*} \right) + \left(I - I^* - I^* \ln \frac{I}{I^*} \right) \\ & + \left(Q - Q^* - Q^* \ln \frac{Q}{Q^*} \right) + \left(R - R^* - R^* \ln \frac{R}{R^*} \right). \end{aligned}$$

The by-product of V along this solution of the model (1) by direct calculation gives:

$$\begin{aligned} \frac{dV}{dt} &= \left(\frac{S - S^*}{S} \right) \frac{dS}{dt} + \left(\frac{V - V^*}{V} \right) \frac{dV}{dt} + \left(\frac{E - E^*}{E} \right) \frac{dE}{dt} \\ &+ \left(\frac{I - I^*}{I} \right) \frac{dI}{dt} + \left(\frac{Q - Q^*}{Q} \right) \frac{dQ}{dt} + \left(\frac{R - R^*}{R} \right) \frac{dR}{dt} \\ &= \left(\frac{S - S^*}{S} \right) [\beta - \alpha(1-x)SI - (1+z)\gamma S - \mu S + \varepsilon V] \\ &+ \left(\frac{V - V^*}{V} \right) [(1+z)\gamma S - (\varepsilon + \mu)V] \\ &+ \left(\frac{E - E^*}{E} \right) [\alpha(1-x)SI - (\rho + \mu)E] \\ &+ \left(\frac{I - I^*}{I} \right) [\rho E - (\tau + \mu + \delta)I] \\ &+ \left(\frac{Q - Q^*}{Q} \right) [\tau(1-\pi)I - (\mu + \delta + k)Q] \\ &+ \left(\frac{R - R^*}{R} \right) [\tau\pi I + kQ - \mu R] \end{aligned}$$

$$\begin{aligned} &= \frac{1}{S} ((S - S^*)\beta - \alpha(1-x)(S - S^*)^2(I - I^*) \\ &\quad - [(1+z)\gamma + \mu](S - S^*)^2 + \varepsilon(V - V^*)(S - S^*)) \\ &\quad + \frac{1}{V} ((1+z)\gamma(S - S^*)(V - V^*) - (\varepsilon + \mu)(V - V^*)^2) \\ &\quad + \frac{1}{E} (\alpha(1-x)(S - S^*)(I - I^*)(E - E^*) \\ &\quad - (\rho + \mu)(E - E^*)^2) + \frac{1}{I} (\rho(E - E^*)(I - I^*) \\ &\quad - (\tau + \mu + \delta)(I - I^*)) + \frac{1}{Q} (\tau(1-\pi)(I - I^*)(Q - Q^*) \\ &\quad - (\mu + \delta + k)(Q - Q^*)^2) + \frac{1}{R} (\tau\pi(I - I^*)(R - R^*) \\ &\quad - k(Q - Q^*)(R - R^*) - \mu(R - R^*)^2) \\ &= -\frac{(S - S^*)^2}{S} \alpha(1-x)(I - I^*) \\ &\quad - \frac{(S - S^*)^2}{S} [(1+z)\gamma + \mu] - \frac{(V - V^*)^2}{V} (\varepsilon + \mu) \\ &\quad - \frac{(E - E^*)^2}{E} (\rho + \mu) - \frac{(I - I^*)^2}{I} (\tau + \mu + \delta) \\ &\quad - \frac{(Q - Q^*)^2}{Q} (\mu + \delta + k) - \frac{(R - R^*)^2}{R} \mu \\ &\quad + \frac{(S - S^*)}{S} \beta + \frac{(S - S^*)}{S} \varepsilon(V - V^*) \\ &\quad + \frac{(V - V^*)}{V} (1+z)\gamma(S - S^*) \\ &\quad + \frac{(E - E^*)}{E} \alpha(1-x)(S - S^*)(I - I^*) \\ &\quad + \frac{(I - I^*)}{I} \rho(E - E^*) + \frac{(Q - Q^*)}{Q} \tau(1-\pi)(I - I^*) \\ &\quad + \frac{(R - R^*)}{R} [\tau\pi(I - I^*) + k(Q - Q^*)] \end{aligned}$$

accumulating both positive and negative terms ; $\frac{dV}{dt} = M - N$, where

$$\begin{aligned} M &= \frac{(S - S^*)}{S} [\beta + \varepsilon(V - V^*)] + \frac{(V - V^*)}{V} (1+z)\gamma(S - S^*) \\ &\quad + \frac{(E - E^*)}{E} \alpha(1-x)(S - S^*)(I - I^*) \\ &\quad + \frac{(I - I^*)}{I} \rho(E - E^*) + \frac{(Q - Q^*)}{Q} \tau(1-\pi)(I - I^*) \\ &\quad + \frac{(R - R^*)}{R} [\tau\pi(I - I^*) + k(Q - Q^*)] \\ N &= \frac{(S - S^*)^2}{S} [\alpha(1-x)(I - I^*) + [(1+z)\gamma + \mu]] \\ &\quad + \frac{(V - V^*)^2}{V} (\varepsilon + \mu) + \frac{(E - E^*)^2}{E} (\rho + \mu) \\ &\quad + \frac{(I - I^*)^2}{I} (\tau + \mu + \delta) + \frac{(Q - Q^*)^2}{Q} (\mu + \delta + k) \end{aligned}$$

if $M < N$, then $\frac{dV}{dt}$ will be negative, $\frac{dV}{dt} = 0$, if and only if $S = S^*, V = V^*, E = E^*, I = I^*, Q = Q^*$, and $R = R^*$. Thus the largest compact invariant set is $\{(S^*, V^*, E^*, I^*, Q^*, R^*) \in \Omega : \frac{dV}{dt} = 0\}$ is just the singleton set $\{T^*\}$ is the Endemic Equilibrium, by LaSalle's Invariant prin-

Table 2. Sensitivity Indices of R_0 to parameters of the model (1)

Parameter	Description	Sensitivity Index (R_0)
α	Effective Contact Rate	+ 1.000000000
β	Transmission Rate	+ 1.000000000
ε	Wane rate of Vaccine	0.6901996944
τ	Exit rate from infectious class	-0.8451619895
x	Acceptance of enlightenment to avoid being exposed	-0.4285714286
δ	Covid-19 Induced death rate	-0.1521291581
γ	Vaccination rate	-0.6910845660
ρ	Exist rate from Exposed Class	0.00255754453
μ	Natural death rate	-1.004381527
z	Acceptance of enlightenment to go for vaccination	-0.1974527331

ple, it implies that T^* is globally asymptotically stable (g.a.s) in Ω if $M < N$. □

3.9. Sensitivity Analysis

The sensitivity indices with respect to the parameter values given in form of:

$$\chi_{R_0}^\beta = \frac{\partial R_0}{\partial \beta} \times \frac{\beta}{R_0}$$

$$R_0 = \frac{\alpha(1-x)\beta\rho(\mu+\varepsilon)}{(\mu+\rho)(\mu+\delta+\tau)\mu(\gamma z + \gamma + \mu + \varepsilon)} \quad (17)$$

The numerical values showing the relative importance of R_0 parameters are shown in Table 2. It can be shown that based on the findings above, α and β have a clear effect on the virus stability. Therefore, by increasing α and β by 1%, R_0 would increase by 1% in influence. There are parameters with positive relation and those with a negative relation. A negative relationship suggests that an increase in the values of the metric would help to reduce the pandemic brutality. While a positive relationship indicates that frequency of the pandemic would be greatly influenced by an increase in the values of those parameters.

3.10. Homotopy Perturbation Method

Homotopy perturbation technique in solving differential equations is shown with the differential equation form:

$$D(u) = k(r), \quad r \in \Omega \quad (18)$$

Subject to the boundary condition

$$B(u, u_n) = 0, \quad r \in \Gamma \quad (19)$$

The general differential operator is denoted as D , and B represent the boundary operator, $K(r)$ is an analytic function, Γ is the boundary of the domain Ω and u_n represent the derivative following the typical path directed externally from Ω . Thus we can write

$$D(u) = L_T(u) + N_T(u) \quad (20)$$

Where $L_T(u)$, $N_T(u)$ represent the linear term, and the nonlinear term of the differential equation respectively. Thus eq. (20) becomes

$$L_T(u) + N_T(u) = k(r) \quad r \in \Omega \quad (21)$$

We can construct a Homotopy for (21) so that

$$H(m, p) = (1-p)[L_T(m) - L_T(u_0)] + p[D(m) - k(r)] = 0 \quad (22)$$

Simplifying this,

$$H(m, p) = L_T(m) - L_T(u_0) + p[L_T(u_0)] + p[N_T(u_0) - k(r)] = 0, \quad (23)$$

where $p \in [0, 1]$ and u_0 denotes the initial approximation. Now, as $p \rightarrow 0$,

$$H(m, 0) = L_T(m) - L_T(u_0) = 0, \quad (24)$$

and as $p \rightarrow 1$,

$$H(m, 1) = D(m) - k(r) = 0.$$

and we can express the solution of the differential equation as

$$M(t) = M_0(t) + pM_1(t) + p^2M_2(t) + \dots \quad (25)$$

Substituting (25) into (3.10) and comparing coefficients of equal powers of p the resulting equation is solved to obtain the value of $M_0(t)$, $M_1(t)$, $M_2(t)$ such that the approximate solution of the differential equation in (18).

$$\lim_{p \rightarrow 1} M(t) = M_0(t) + M_1(t) + M_2(t) + \dots \quad (26)$$

3.11. Application of Homotopy Perturbation Method

Here, the homotopy perturbation approach is used to approximate the solution to differential equation 1 in this section. Procedure (55-63) is constructing a homotopy for model (1)

$$\begin{aligned} \frac{dS}{dt} &= p(\beta - \alpha(1-x)SI - (1+z)\gamma S - \mu S + \varepsilon V), \\ \frac{dV}{dt} &= p((1+z)\gamma S - (\mu + \varepsilon)V), \\ \frac{dE}{dt} &= p(\alpha(1-x)SI - (\rho + \mu)E), \\ \frac{dI}{dt} &= p(\rho E - (\tau + \mu + \delta)I), \\ \frac{dQ}{dt} &= p(\tau(1-\pi)I - (\mu + \delta + k)Q), \\ \frac{dR}{dt} &= p(\tau\pi I + kQ - \mu R). \end{aligned} \quad (27)$$

Subject to initial conditions $S(0) = s_0$, $E(0) = e_0$, $I(0) = i_0$, $Q(0) = q_0$, $R(0) = r_0$. The following system of powers series

are assumed to be the solution to problem (1)

$$\begin{aligned}
 S(t) &= s_0(t) + ps_1(t) + p^2s_2(t) + \dots \\
 V(t) &= v_0(t) + pv_1(t) + p^2v_2(t) + \dots \\
 E(t) &= e_0(t) + pe_1(t) + p^2e_2(t) + \dots \\
 I(t) &= i_0(t) + pi_1(t) + p^2i_2(t) + \dots \\
 Q(t) &= q_0(t) + pq_1(t) + p^2q_2(t) + \dots \\
 R(t) &= r_0(t) + pr_1(t) + p^2r_2(t) + \dots
 \end{aligned}
 \tag{28}$$

Substituting these values into each compartment of (27) and comparing the coefficients of equal powers of p , the following results were generated for each compartment when the initial values were applied.

$$\begin{aligned}
 p^0 : \frac{ds_0(t)}{dt} &= 0, \quad \frac{dv_0(t)}{dt} = 0, \quad \frac{di_0(t)}{dt} = 0, \\
 \frac{de_0(t)}{dt} &= 0, \quad \frac{dq_0(t)}{dt} = 0, \quad \frac{dr_0(t)}{dt} = 0.
 \end{aligned}
 \tag{29}$$

Solving for each of the classes in (29), the following are obtained as first iterations.

$$\begin{aligned}
 s_0(t) &= s_0, \quad v_0(t) = v_0, \quad i_0(t) = i_0, \quad e_0(t) = e_0, \\
 q_0(t) &= i_0, \quad r_0(t) = r_0,
 \end{aligned}
 \tag{30}$$

Also, the coefficient of p^1 is given as

$$\begin{aligned}
 p^1 : \frac{ds_1}{dt} &= \beta - \alpha(1-x)S_0(t)I_0(t) - (1+z)\gamma S_0(t) \\
 &\quad - \mu S_0(t) + \varepsilon V_0(t) \\
 \frac{dv_1}{dt} &= (1+z)\gamma S_0(t) - (\mu + \varepsilon)VS_0(t) \\
 \frac{de_1}{dt} &= \alpha(1-x)S_0(t)I_0(t) - (\rho + \mu)E_0(t) \\
 \frac{di_1}{dt} &= E_0(t) - (\tau + \mu + \delta)I_0(t) \\
 \frac{dq_1}{dt} &= \tau(1-\pi)I_0(t) - (\mu + \delta + k)Q_0(t) \\
 \frac{dr_1}{dt} &= \tau\pi I_0(t) + kQ_0(t) - \mu R_0(t).
 \end{aligned}$$

Solving this system of equation yields

$$\begin{aligned}
 s_1(t) &= (\beta - \alpha(1-x)S_0I_0 - (1+z)\gamma S_0 - \mu S_0 + \varepsilon V_0)t \\
 v_1(t) &= ((1+z)\gamma S_0 - (\mu + \varepsilon)VS_0)t \\
 e_1(t) &= (\alpha(1-x)S_0I_0 - (\rho + \mu)E_0)t \\
 i_1(t) &= \rho(E_0 - (\tau + \mu + \delta)I_0)t \\
 q_1(t) &= (\tau(1-\pi)I_0 - (\mu + \delta + k)Q_0)t \\
 r_1(t) &= (\gamma i_0 - (\mu + \delta)r_0)t
 \end{aligned}$$

Similarly comparing the coefficients of p^2 ;

$$\begin{aligned}
 p^2 : \frac{ds_2}{dt} &= \beta - \alpha(1-x)S_1(t)I_1(t) - (1+z)\gamma S_1(t) \\
 &\quad - \mu S_1(t) + \varepsilon V_1(t) \\
 \frac{dv_2}{dt} &= (1+z)\gamma S_1(t) - (\mu + \varepsilon)VS_1(t)
 \end{aligned}$$

$$\begin{aligned}
 \frac{de_2}{dt} &= \alpha(1-x)S_0(t)I_0(t) - (\rho + \mu)E_0(t) \\
 \frac{di_2}{dt} &= \rho E_1(t) - (\tau + \mu + \delta)I_1(t) \\
 \frac{dq_2}{dt} &= \tau(1-\pi)I_1(t) - (\mu + \delta + k)Q_1(t) \\
 \frac{dr_2}{dt} &= \tau\pi I_1(t) + kQ_1(t) - \mu R_1(t)
 \end{aligned}$$

Solving this system of differential equation, the results are obtained.

The third iterations are similarly obtained and the solution for each class is obtained by taking the sum of its approximations. That is

$$\begin{aligned}
 S(t) &= \sum_{n=0}^3 s_n(t), \quad v(t) = \sum_{n=0}^3 v_n(t), \quad E(t) = \sum_{n=0}^3 e_n(t), \\
 I(t) &= \sum_{n=0}^3 i_n(t), \quad Q(t) = \sum_{n=0}^3 q_n(t), \quad R(t) = \sum_{n=0}^3 r_n(t).
 \end{aligned}$$

Evaluating the obtained results substituting the following values for their respective parameters,

The following series results embedding the acceptance of enlightenment to go for vaccination (z) are obtained for each of the class; such that

$$\begin{aligned}
 S(t) &= 50 + (-20.0 - 49.26192564z)t \\
 &\quad + (67.44190644 + 8z^2 + 50.52954051z)\frac{t^2}{2} \\
 &\quad + (-111.2084361 - 3.20z^3 - 32.54172431z^2 \\
 &\quad - 100.5680654z)\frac{t^3}{6} \\
 V(t) &= 22 + (14.49294872 + 20.0z)t \\
 &\quad - (32.71118051z + 8.00z^2 + 23.33265261)\frac{t^2}{2} \\
 &\quad + (55.37685825z + 25.41438031z^2 \\
 &\quad + 32.81740413 + 3.2z^3)\frac{t^3}{6} \\
 E(t) &= 12 + 42.98205385t - (17.8183600z - 49.69955324)\frac{t^2}{2} \\
 &\quad - (-47.50759391z + 7.12734400z^2 - 84.85376560)\frac{t^3}{6} \\
 I(t) &= 14 - 0.0659282048t + 2.809424028\frac{t^2}{2} \\
 &\quad - (6.463168788 + 2.316386800)\frac{t^3}{6} \\
 Q(t) &= 16 - 0.306838205t - 0.01095678148t^2 \\
 &\quad + 0.07378498873t^3 \\
 R(t) &= 5 + 1.178300333t - 0.01108080588t^2 \\
 &\quad + 0.004209859285t^3
 \end{aligned}$$

Similarly, the results obtained for the acceptance of enlightenment to avoid being exposed (x) for each class $S(t), V(t), \dots, R(t)$

$$S(t) = 50 + (-74.35302564 + 63.63700x)t$$

$$\begin{aligned}
 &+ (-209.0367384x + 80.99335540x^2 \\
 &+ 138.7423881)\frac{t^2}{2} + (-297.4348082 \\
 &- 635.7511634x - 449.6422846x^2 \\
 &+ 103.0834832x^3)\frac{t^3}{6} \\
 V(t) = &22 + (20.49294872)t - (-33.0912400x \\
 &+ 43.79337876)\frac{t^2}{2} + (83.10842284 \\
 &+ 42.11654480x^2 - 116.9825201)\frac{t^3}{6} \\
 E(t) = &12 + (2.07315385 - 63.63700x)t \\
 &- (184.2183084x - 80.99335540x^2 \\
 &- 103.0211518)\frac{t^2}{2} - (542.7196750x \\
 &- 418.0548761x^3 + 103.0834832x^3 \\
 &- 227.7217222)\frac{t^3}{6} \\
 I(t) = &14 - 0.065928205t - (8.100691055 \\
 &- 8.2728100x)\frac{t^2}{2} - (-23.94838008x \\
 &+ 10.52913620x^2 + 13.39497658)\frac{t^3}{6} \\
 Q(t) = &16 - 0.3068382048t - 0.01095678145t^2 \\
 &+ (0.6546688194x - 0.6391105783)\frac{t^3}{6} \\
 R(t) = &5 + 1.178300333t - 0.005742708942xt^3 \\
 &- 0.01108080587t^2 + 0.005932671968t^3
 \end{aligned}$$

4. Graphical Results

After evaluating series of result using the baseline parameter from Table 1. The results are shown graphically. Figures 2 and 3 reveal the impact of acceptance of enlightenment to avoid being exposed on the susceptible and exposed classes. In Figure 2, it could be observed that the number of susceptible individuals tends to increase as they avoid being exposed to COVID-19 through contact with the infected group. Transitivity, the exposed class, as shown in Figure 3, confirmed that the higher the rate of acceptance to avoid getting exposed increases, the lower the exposed population reduces with time.

5. Discussion of Results

An elaborate numerical technique is used to support the analytic results and explore the influence of model parameters like the rate of enlightenment acceptance to avoid exposure and the rate of enlightenment acceptance to go for vaccination. We choose baseline parameter values that are compatible with the spread of COVID-19 infection and transmission. Under conditions of low basic reproduction numbers, the disease-free equilibrium is locally asymptotically stable, i.e., $R_0 < 1$. COVID-19 persists in the population if $R_0 > 1$. Figure 4 depicts the increase in the acceptance rate of enlightenment to go for vaccination in susceptible classes. Figure 5 also depicts the acceptance rate of enlightenment to vaccination in the vaccinated class. The

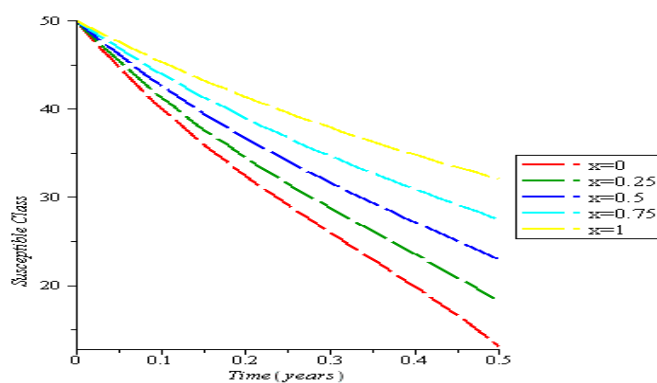


Figure 2. Graph illustrating the effect of a change in x on susceptible class

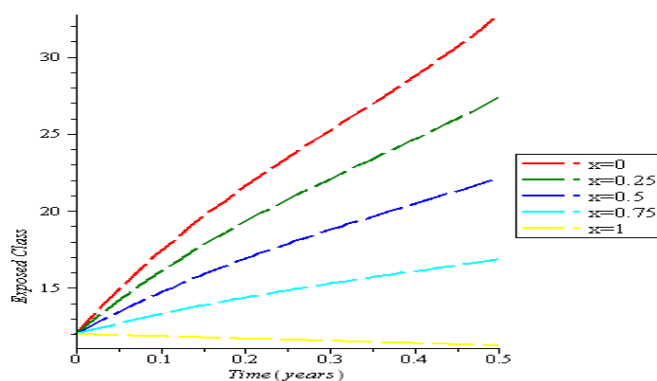


Figure 3. Graph showing the impact of variation of x on the exposed class

influence of the acceptance rate of enlightenment to avoid being exposed is shown in Figures 2 and 3.

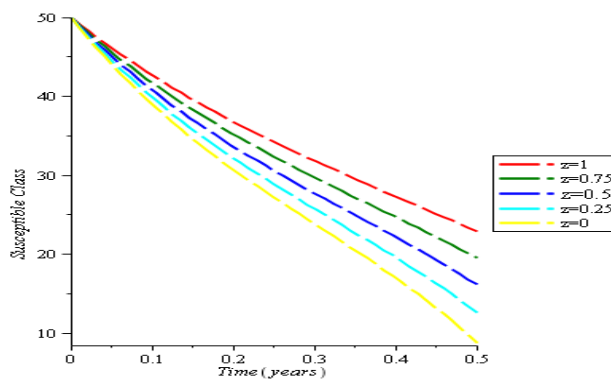


Figure 4. Shows the variation of z , that is, the acceptance of enlightenment to go for vaccination on the susceptible class. As the rate of acceptance enlightenment to go for vaccination increases the number of susceptible individual also increases with time

6. Conclusion

This study developed and analyzed a mathematical model of COVID-19 transmission dynamics with an agreed enlightenment rate. Analyzing the model on a theoretical and numerical level, it was shown that if the fundamental reproduction number is less than one, the disease-free equilibrium is asymptoti-

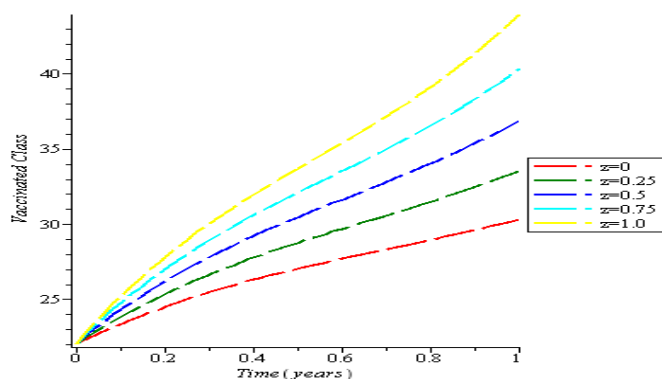


Figure 5. Graph shows the effect of acceptance of enlightenment for vaccination. It reveals that as the rate increases, the vaccinated individuals also increased

cally stable on both a local and a global scale. If the basic reproduction number is greater than one, COVID-19 illness persists in the community. It has been shown that the transmission rate has a considerable influence on the spread of COVID-19. This was determined by doing a sensitivity study. Every effort should be made to avoid unnecessary transmission among COVID-19 infected individuals. COVID-19 infection rates will be reduced if the general population is more accepting of information about the disease. This research also emphasized the need for educating people about vaccinations in order to avoid and control the development of COVID-19. The most effective way to reduce the spread of COVID-19 is to raise awareness among the general public about the importance of routine immunizations such as the first, second, and booster doses.

Acknowledgement. The authors would like to acknowledge the efforts of the entire staffs of the Department of Mathematical Sciences, Osun State University, Osogbo, Nigeria.

Conflict of interest. No conflict of interest is reported by the author in publishing this paper.

References

- [1] K. Roosa, Y. Lee, R. Luo, A. Kirpich, R. Rothenberg, J. Hyman, P. Yan, and G. Chowell, "Real-time forecasts of the COVID-19 epidemic in China from February 5th to February 24th, 2020," *Infectious Disease Modelling*, vol. 5, pp. 256–263, 2020. DOI: 10.1016/j.idm.2020.02.002
- [2] O. A. Adegboye, A. I. Adekunle, and E. Gayawan, "Early transmission dynamics of novel Coronavirus (COVID-19) in Nigeria," *International Journal of Environmental Research and Public Health*, vol. 17, no. 9, p. 3054, 2020. DOI: 10.3390/ijerph17093054
- [3] M. V. Krishna and J. Prakash, "Mathematical modelling on phase based transmissibility of Coronavirus," *Infectious Disease Modelling*, vol. 5, pp. 375–385, 2020. DOI: 10.1016/j.idm.2020.06.005
- [4] N. Ferguson et al., "Impact of non-pharmaceutical interventions (NPIs) to reduce COVID-19 mortality and healthcare demand," *Imperial College London*, 2020. DOI: 10.25561/77482
- [5] T. A. Ayoola, M. K. Kolawole, and A. O. Popoola, "Mathematical Model of COVID-19 Transmission Dynamics with Double Dose Vaccination," *Tanzania Journal of Science*, vol. 48, no. 2, pp. 499–512, 2022. DOI: 10.4314/tjs.v48i2.23
- [6] X. Wang, "Studying social awareness of physical distancing in mitigating COVID-19 transmission," *Mathematical Biosciences and Engineering*, vol. 17, no. 6, pp. 7428–7441, 2020. DOI: 10.3934/mbe.2020380
- [7] M. A. Balya et al., "Investigating the Impact of Social Awareness and Rapid Test on A COVID-19 Transmission Model," *Communication in Biomathematical Sciences*, vol. 4, no. 1, pp. 46–64, 2021. DOI: 10.5614/cbms.2021.4.1.5
- [8] S. S. Musa, S. Qureshi, S. Zhao, A. Yusuf, U. T. Mustapha, and D. He, "Mathematical modeling of COVID-19 epidemic with effect of awareness programs," *Infectious Disease Modelling*, vol. 6, pp. 448–460, 2021. DOI: 10.1016/j.idm.2021.01.012
- [9] G. Adomian, "A review of the decomposition method and some recent results for nonlinear equations," *Computers & Mathematics with Applications*, vol. 21, no. 5, pp. 101–127, 1991. DOI: 10.1016/0898-1221(91)90220-X
- [10] J.-H. He, "Variational iteration method – a kind of non-linear analytical technique: some examples," *International Journal of Non-Linear Mechanics*, vol. 34, no. 4, pp. 699–708, 1999. DOI: 10.1016/S0020-7462(98)00048-1
- [11] J.-H. He, "Homotopy perturbation technique," *Computer Methods in Applied Mechanics and Engineering*, vol. 178, no. 3-4, pp. 257–262, 1999. DOI: 10.1016/S0045-7825(99)00018-3
- [12] S. Balamuralitharan and S. Geethamalini, "Solutions of the epidemic of EIAV infection by HPM," *Journal of Physics: Conference Series*, vol. 1000, no. 1, p. 012023, 2018. DOI: 10.1088/1742-6596/1000/1/012023
- [13] A. Alaje, M. Olayiwola, M. Ogunniran, J. Adediji, and K. Adedokun, "Approximate Analytical methods for the solution of Fractional Order Integro-differential equation," *Nigerian Journal of Mathematics and Applications*, vol. 31, p. 175, 2021.
- [14] O. Chandrow, "Forecasting COVID-19 pandemic in Bangladesh by using Homotopy perturbation Method," *Journal of Mathematics (IOSR-JM)*, 2021.
- [15] M. M. Jumanne and S. Z. Naboth, "Mathematical Model of COVID-19 transmission Dynamics and Control Strategies," *Journal of Applied and Computation Math*, vol. 9, 2020.
- [16] B. Tang, X. Wang, Q. Li, N. L. Bragazzi, S. Tang, Y. Xiao, and J. Wu, "Estimation of the Transmission Risk of the 2019-nCoV and Its Implication for Public Health Interventions," *Journal of Clinical Medicine*, vol. 9, no. 2, p. 462, 2020. DOI: 10.3390/jcm9020462
- [17] A. Babaei, H. Jafari, S. Banihashemi, and M. Ahmadi, "Mathematical analysis of a stochastic model for spread of Coronavirus," *Chaos, Solitons & Fractals*, vol. 145, p. 110788, 2021. DOI: 10.1016/j.chaos.2021.110788
- [18] C. T. Deressa, Y. O. Mussa, and G. F. Duressa, "Optimal control and sensitivity analysis for transmission dynamics of Coronavirus," *Results in Physics*, vol. 19, p. 103642, 2020. DOI: 10.1016/j.rinp.2020.103642
- [19] S. M. Garba, J. M.-S. Lubuma, and B. Tsanou, "Modeling the transmission dynamics of the COVID-19 Pandemic in South Africa," *Mathematical Biosciences*, vol. 328, p. 108441, 2020. DOI: 10.1016/j.mbs.2020.108441
- [20] M. Yavuz, F. Ö. Coşar, F. Günay, and F. N. Özdemir, "A New Mathematical Modeling of the COVID-19 Pandemic Including the Vaccination Campaign," *Open Journal of Modelling and Simulation*, vol. 09, no. 03, pp. 299–321, 2021. DOI: 10.4236/ojmsi.2021.93020
- [21] J. Zhang, J. Dean, Y. Yin, D. Wang, Y. Sun, Z. Zhao, and W. J., "Determinants of covid-19 vaccine acceptance and hesitancy: a health care student - based online survey in northwest china." *Frontiers in Public Health*, vol. 9, 2022. DOI: 10.3389/fpubh.2021.777565
- [22] O. Diekmann and J. Heesterbeek, *Mathematical Epidemiology of Infectious Diseases: Model Building, Analysis and Interpretation*, ser. Wiley Series in Mathematical & Computational Biology. Wiley, 2000. ISBN 9780471492412.
- [23] C. Castillo-Chavez and B. Song, "Dynamical Models of Tuberculosis and Their Applications," *Mathematical Biosciences and Engineering*, vol. 1, no. 2, pp. 361–404, 2004. DOI: 10.3934/mbe.2004.1.361